STUDY OF BOUNDARY LAYER FLOW IN ROTATING CURVATURE SYSTEM (THE OCCURRENCE AND GROWTH OF STREAMWISE VORTICES)

Yutaka Hasegawa
Research Center for Advanced Energy Conversion, Nagoya University
Furo-cho, Chikusa-ku, Nagoya 464-8603, Japan
hasegawa@mech.nagoya-u.ac.jp

Koji Kikuyama, Michio Nishikawa, and Takahiro Ikeda
Department of Mechanical Engineering, Nagoya University
Furo-cho, Chikusa-ku, Nagoya 464-8603, Japan
kikuyama@mech.nagoya-u.ac.jp, michio-n@mbox.nagoya-u.ac.jp

ABSTRACT

The behavior of the boundary layer in rotating channels, such as that in impeller passages of turbomachinery, is dominantly influenced by the centrifugal and Coriolis forces due to the wall curvature and system rotation, respectively. The resultant force may promote or suppress the instability in the boundary layer, depending on its magnitude of the component normal to the wall boundary.

The purpose of the present study is to make clear experimentally the effects of Görtler type instability on the laminar boundary layer developing along the concave surface, focusing attention on transition process from laminar to turbulent state in the rotating system with streamline curvature. The longitudinal velocity and turbulent intensity have been measured near the concave surface in the channel whose radii of center line curvature is 1,000mm. When the Coriolis force acts toward the concave wall due to the channel rotation, the occurrence of the Görtler vortices shifts upstream and the vortex structure is maintained in more downstream sections. In the earlier stage of vortex development an oscillation of flow was found to appear in the vortices despite of the rotating condition.

1. INTRODUCTION

A detailed knowledge of the flow pattern inside the impeller passage is imperative for the design and performance prediction of the turbomachinery. The fluid motion in the impeller is subject to the body forces due to the rotation and curvature of the channel, which results in the complicated three-dimensional boundary layer developing on the impeller blades and sidewalls. One of the keen issues for improving the impeller efficiency is to control the boundary layer condition such as the transition.

The effects of system rotation or wall curvature on the turbulent boundary layer have been examined by some experimental studies(1973)(1979)(1987), and Bradshaw(1969) showed a similar relationship between the centrifugal force in a curved channel and the Coriolis force in a rotating straight channel. It has been also found that the fluctuating components in the turbulent boundary layer are promoted on the pressure side, and suppressed on the suction side due to these body forces.

The experimental studies on the laminar boundary layer have been done, about the occurrence of the longitudinal vortices and the transition to turbulent in the rotating straight channel(1990), and about the effects of Coriolis force on the instability of the laminar boundary layer flowing along the rotating flat plate(1991). Numerical analyses for the instability of the laminar boundary layer in the rotating curvature system have been done based on the linear stability theory(1993)(1996)(2000). However, there have been few experimental works about the boundary layer transition on the rotating curved system such as blade surface in the centrifugal impeller.

The present authors performed a series of experiments for the boundary layer in the rotating curved system by measuring the time-mean velocity profiles as well as the fluctuating components(2002), and the following results has been obtained. The transition triggered by Görtler type instability is promoted on the pressure side and delayed on the suction side, due to the resultant effects from the centrifugal and Coriolis forces. A key parameter for the boundary layer transition is Görtler number defined by the momentum thickness and the radius of wall curvature. It was also found that the boundary layer flow in the transition stage possesses periodic fluctuations in the time domain as well as the space domain.

This paper aims at clarifying the effects of system rotation on the boundary layer transition due to Görtler type instability on the rotating concave surface, and describes the changing structure of longitudinal vortices measured by a multi-probe hot wire system.

2. EQUIPMENT AND METHOD OF EXPERIMENT

Figure 1 shows a schematic outline of the experimental equipment. Two channels of different radii of curvature, R=1,000mm and 2,000mm, are shown to be settled on a rotation table of 3,000mm in diameter. In the present study only the channel of R=1,000mm was used. The rotating table sup-

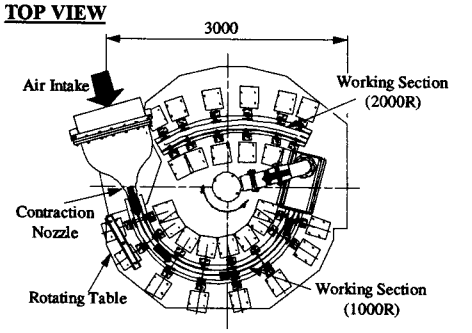

(a) Top view

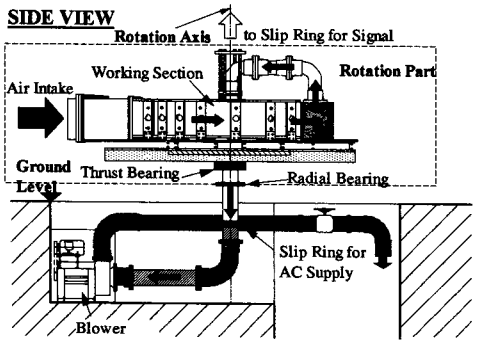

(b) Side view

Fig.1 Schematic outline of experimental equipment

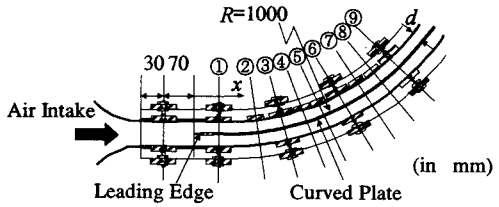

Fig.2 Measurement sections in curved channel

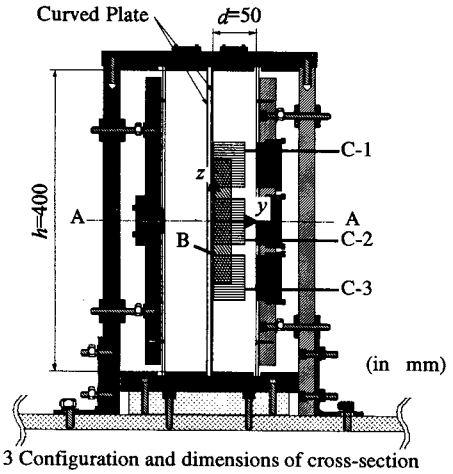

Fig. 3 Configuration and dimensions of cross-section

ported by thrust bearings can rotate both in the clockwise and anti-clockwise directions around the vertical axis in Fig.1(b), so as to change the direction of the Coriolis force. Air was introduced into the curved channel through a two-dimensional nozzle and exhausted outside through the hollow rotating axis by a blower settled in a stationary system.

Figure 2 shows the upstream measurement sections in the channel of R = 1,000mm. In order to get rid of the effects of the upstream boundary layer developing inside the contraction nozzle, a thin stainless plate was inserted along the center line of the channel. As the flow just upstream of the leading edge of the plate was ascertained to be uniform, measurements of the velocity and turbulence were made in the boundary layer developing along the concave surface of the plate.

Table 1 Longitudinal distance of measurement sections

Section Number	Streamwise distance of measurement section (x/d)	(1)The section measured by single-probe	(2)The section measured by multi-probes
Sec.1	2.6	O	O
Sec.2	5.41		O
Sec.3	8.21	O	O
Sec.4	10.81		O
Sec.5	13.42		O
Sec.6	16.02	O	O
Sec.7	18.63		O
Sec.8	21.23		O
Sec.9	23.84	O	O
Sec.10	26.44		O
Sec.11	29.05		O
Sec.12	31.65	O	O
Sec.13	39.47	O	O
Sec.14	47.28	O	O

Figure 3 shows the configuration of a measurement section. The high aspect ratio h/d of 8:1 was employed so as to avoid the effects of the top and the bottom walls on the flow in the central region of the section. The longitudinal distances of the measuring sections from the leading edge of the plate are listed in Tab.1 for the channel of R=1,000mm. The Reynolds number based on the free stream velocity in Sec. 1, U_m, and the channel width, d, $Re = U_m d/\nu$, was taken to be 1.8×10^4 and the dimensionless rotation rate, N, defined by the following relation was taken to be 0, ±0.012, where the sign of N denotes the rotational direction of channels, that is, the positive value corresponds to the direction where the Coriolis force acts toward the concave wall.

$$N = d\Omega/U_m \qquad (1)$$

In the case of N=0.012, the ratio between centrifugal force due to wall curvature and Coriolis force due to system rotation is about 2:1.

3.EXPERIMENTAL RESULTS AND DISCUSSIONS

3.1 Velocity and turbulent intensity distribution

In order to investigate the changes of the flow pattern along the concave boundary toward longitudinal direction, time averaged velocity and turbulent intensity were measured at 24 points of spanwise direction in each cross section. Figure 4 shows the profiles of velocity and turbulent intensity at the sections shown in the Tab.1 the column (1), which are averaged to spanwise direction. U_m is free stream velocity at Sec.1 just after the entrance of the channel. The effect of the channel rotation does not apparently reflect on the averaged velocity profiles, except for the boundary layer at Sec.6, which is in transition process to turbulent. When both the Coriolis force due to the system rotation and the centrifugal force due to the wall curvature act toward the concave wall, that is, in case of the N=0.012, turbulent intensity near the wall at Sec.6 increases in comparison with the stationary condition of N=0. This can be attributed to enhancement of the Görtler type instability, and the turbulent intensity was suppressed in case of N=-0.012, when the Coriolis and centrifugal forces act in the opposite direction. In Secs. 12~14, turbulent boundary layer is fully developed, and there is again a little difference in the profile by rotation rates.

Figure 5 shows the changes of the momentum thickness

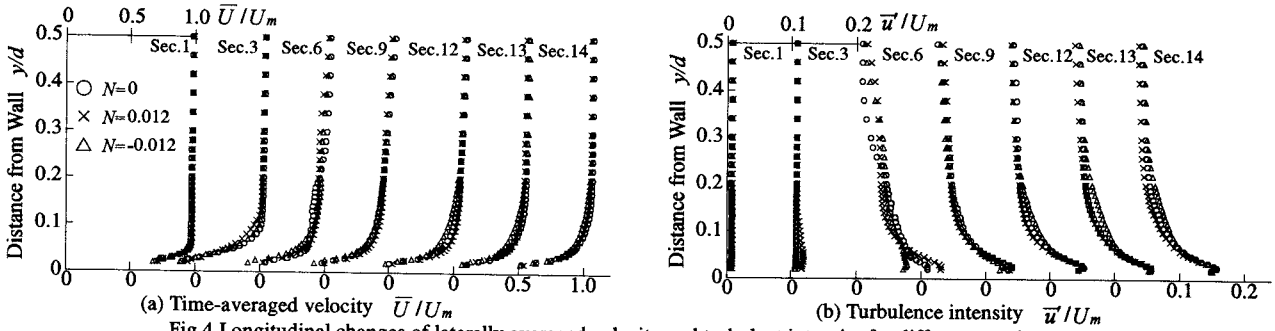

Fig.4 Longitudinal changes of laterally averaged velocity and turbulent intensity for different rotation rates

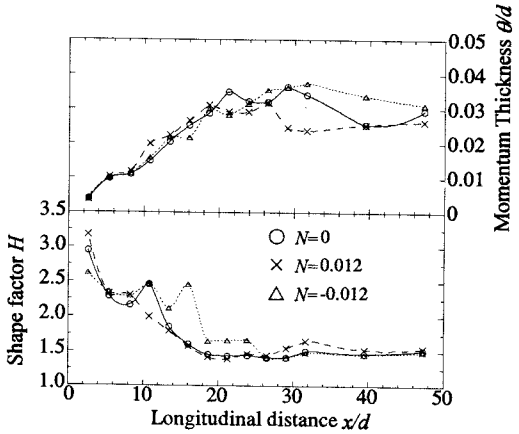

Fig. 5 Variations of boundary layer thickness and shape factor

θ and shape factor H given by the velocity profile in the section. The momentum thickness increases almost in the same manner for all rotation rates until the boundary layer transition completes. When the turbulent state is fully developed (x/d>30), the boundary layer thickness differs by the rotation rates because of the different velocity gradient in the outer flow region, which is in balance with the effects from the rotation rate and wall curvature as a channel flow. From the results of the shape factor, it can be confirmed that the transition is delayed in the case of N=-0.012 compared with the other conditions. This is because the fluctuating component was suppressed by the decrease of Görtler type instability, and boundary layer is kept laminar in longer distance along the concave wall. After the boundary layer transition, the shape factor H takes almost constant value about 1.4.

3.2 Longitudinal change in vortex structure

In order to confirm the occurrence of Görtler vortices and to understand their structure, the velocity measurement using single hot wire probe has been done at the seven sections shown in the column (1) of Tab.1. The measurement area in each section locates in the spanwise direction z/d=-0.2~0.2 and the normal direction to the wall y/d=0.05~0.40 (8 points of 0.05 interval). The contour plots of the time-averaged velocity U/U_m are shown in Fig.6.

For the rotation rate N=0 shown in Fig. 6(a), an almost uniform flow is introduced into Sec.1, close to the channel entrance, whose turbulent intensity is about 1% as shown in Fig. 4. At Sec.3 small distortion of the velocity profile can be found in the close vicinity of the concave wall and locally retarded regions exist at some spanwise positions such as z/h=-0.15 and 0.12. It indicates the occurrence of the ejection, which brings the retarded fluid elements in the boundary layer into high-speed outer region. At Sec.6 located in transition process, there are high and low velocity regions alternately located in the spanwise direction inside the boundary layer, and it can be said that longitudinal vortices are detected on the concave wall by the velocity measurement. At Sec.9, where turbulent boundary layer is developing, the effect of longitudinal vortices extends over the boundary layer into the outer region, the number of vortices pairs decreased and their spanwise width is increased in comparison with the upstream section Sec.6. As the turbulent boundary layer develops downstream, the distribution tends to be uniform in the spanwise direction due to increase of turbulent mixing, although the vortex structure seems to be kept even in the turbulent state.

Figures 6(b) and (c) show the time-averaged velocity distributions in the cross sections for the rotation rates N=0.012 and -0.012, respectively. For N=0.012, the velocity distortion near the wall appears more clearly, which suggests enhanced development of Görtler vortices and thus the stronger ejection due to the system rotation, if compared with stationary state N=0. This result agrees qualitatively well with the numerical analysis based on the linear stability theory. At Sec.6, the effects of the Görtler vortices penetrate through the boundary layer into the outer region. As the flow goes downstream, the number of vortices pairs decreases and the retarded regions move away from the center of swanwise position.

In case of N=-0.012, distortion of velocity profile becomes noticeable from Sec.3. The configuration of the retarded regions, thus the Görtler vortices, seems to be irregular at Sec.6, and it can be attributed to the decreased resultant force, which promotes the Görtler type instability. Although the number of the vortices pairs decreases in the downstream sections as the same as the other rotating conditions, the interval of the vortices pair seems to be constant from Sec.12 to Sec.14 in contrast to the rotation rate N=0.012.

From the velocity distributions shown in Fig.6, the inception of the Görtler vortices and the increase of its interval toward flow direction can be determined for the different rotation rates. Figure 7 summarizes the streamwise change in the vortices pitch λ which is averaged over the measurement area (-0.2<z/h<0.2) and normalized by the channel width. For every rotation rate, the pitch is kept almost unchanged in the laminar state region, and increases rapidly in the transition process. After the transition, increasing rate of the pitch become smaller, especially in the case of N=-0.012, when the resultant force toward the wall is smaller than the other rotation rates.

3.3 Unsteady behavior of Görtler vortices

The previous section described the occurrence of Görtler vortices in the boundary layer flow on rotating concave sur-

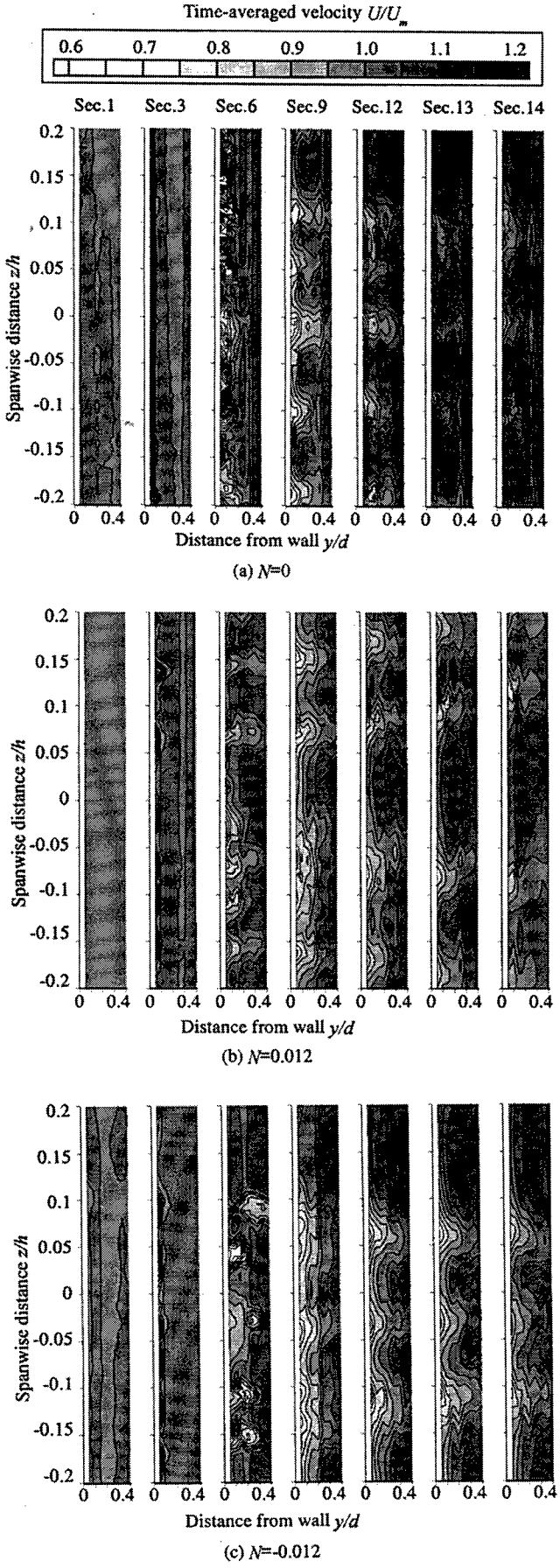

Fig.6 Time-averaged velocity distributions in the region of B (in Fig. 3), for (a)N=0, (b)N=0.012 and (c)N=-0.012

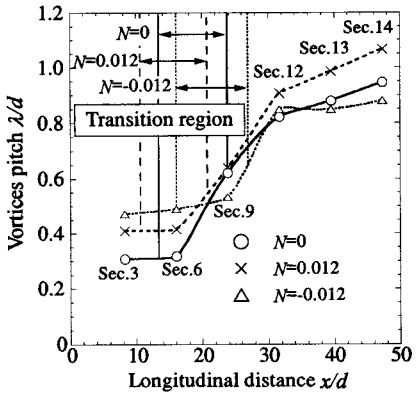

Fig.7 Downstream changes of vortices pitch

face and the development of the vortices with changing structure in the transition process. In order to examine the behavior of Görtler vortices more in detail, simultaneous velocity measurement has been done adopting a multi-probe system, which has 8 hot-wire probes (Wire positions 1~8) aligned in spanwise direction with 7 mm intervals. The system can be traversed in y-direction and covers the measurement regions of C-1, 2 and 3 shown in Fig.3 in each cross section. Figure 8 shows the time-averaged velocity distributions U/U_m obtained in C-1 at measurement sections Secs.3~9 for N=0.012. The result consists with Fig.6(b) obtained by using a single probe, showing the low velocity regions located at about z/h=0.14 and 0.2.

The power spectra are shown in Fig.9 for the low velocity region (see Fig.8) retarded by the ejection due to the longitudinal vortices, in the transition region, Secs.3~6. The measurement locations correspond to the wire position 3 (at z/h=0.20) at respective distances from the wall as shown by the dashed lines in Fig.8. At Sec.3, where the distortion in the velocity profile comes out near the wall, there are no dominant fluctuations except for very small peaks about 400 and 2400Hz. A striking peak around 400Hz can be found in Sec.4, where the Görtler vortices have developed rapidly. There is the same trend in the spectrum throughout the boundary layer, although the strength varies with the positions. In the downstream, at Sec.5 and 6, the power spectra are similar to those of fully turbulent flows without any particular dominant fluctuation.

The distributions of the time averaged velocity are shown in Fig.10 for the rotation rate N=-0.012, at Secs.4, 5, and 6 in the region C-2. The development of Görtler vortices is delayed, and the shape of the retarded regions becomes irregular compared with the case for N=0.012 due to less resultant force to the wall direction. The power spectra for N=-0.012 are shown in Fig.11 measured at Pos.1 and 4 in Secs.4, 5, and 6. In Sec. 4, there is a spike in the spectrum for Pos.1 and 4 around 400Hz, which is almost the same frequency as the peak found in the case of N=0.012. Thus, it can be considered that this is a kind of velocity disturbance inherent in the initial stage of the Görtler type instability. In Secs. 5 and 6, at Pos.1, the profile of the power spectrum approaches to those of the turbulent state and shows a peak around 100 Hz, while at Pos. 4 the spike around 400 Hz still remains in Sec.5 and possesses a peak around 200 Hz in Sec.6. In contrast to the upstream section, the characteristic frequency of the velocity fluctuation varies over the cross section, and this can be related to the irregular shape of the retarded region, thus the incomplete structure of the longitudinal vortices generated

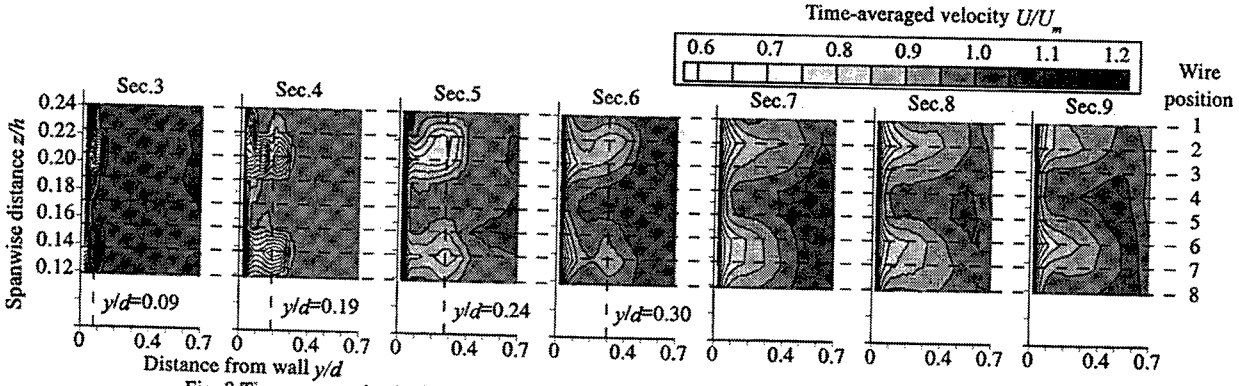

Fig. 8 Time-averaged velocity distributions for N=0.012, at Sec.3-9, in the region of C-1 (in Fig.3)

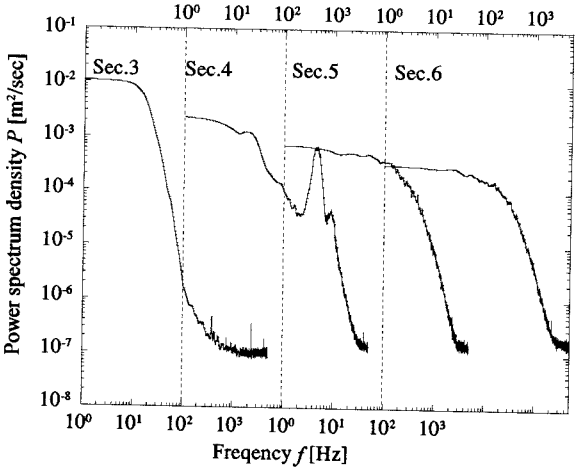

Fig.9 Power spectrum of fluctuating component at wire position 3, Sec.3(y/d=0.09) , Sec.4 (y/d=0.19), Sec.5 (y/d=0.24) and Sec.6 (y/d=0.3) for N=0.012

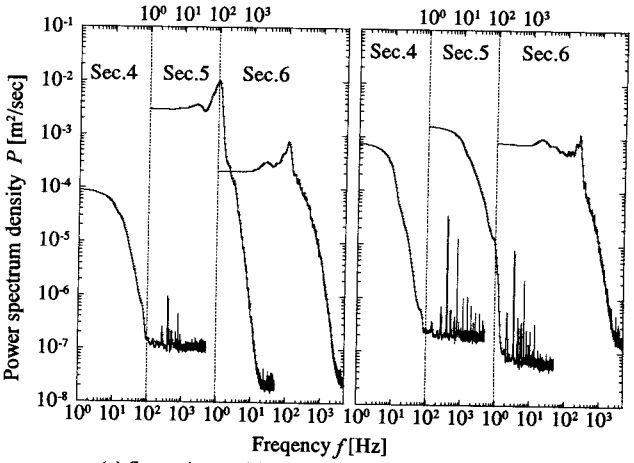

(a) Spanwise position 1 (b) Spanwise position 4

Fig.11 Power spectrum of fluctuating component for N=-0.012
(a) pos.1, Sec.4 (y/d=0.09), Sec.5 (y/d=0.22) and Sec.6 (y/d=0.24)
(b) pos.4, Sec.4 (y/d=0.09), Sec.5 (y/d=0.1) and Sec.6 (y/d=0.14)

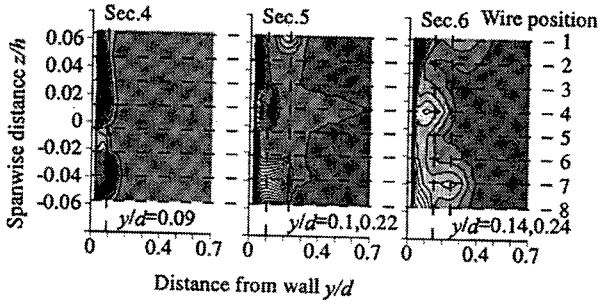

Fig. 10 Time-averaged velocity distribution for N=-0.012, at Sec.4-6, in the region of C-2 (in Fig.3)

for N=-0.012. In the boundary layer on the concave surface, the velocity fluctuation seems to occur depending deeply on the shape of Görtler vortices during the transition process.

Time traces of the instantaneous velocity profile at the locations indicated by the dashed lines in Figs. 8 and 10 are shown in Figs.12, and 13, for N=0.012 and -0.012, respectively. The steady flow structure can be seen in Figs.12(a) and13(a), although the power spectra in the low speed region possess a spike around the same frequency of 400Hz.

Downstream in Sec.4 for N=0.012 and Sec.5 for N=-0.012, where the longitudinal vortex structure has expanded in the spanwise and normal directions, the velocity fluctuation occurs periodically at the retarded region. At the wire positions 2 and 3 in Fig.12(b), the velocity fluctuates alternately with the frequency of about 400Hz, while the fluctuation with slightly lower frequency than 400Hz appears at the position 7. For rotation rate N=-0.012, in Sec.5 (Fig.13(b)), the retarded flow at Pos.1 has the velocity fluctuation around 100 Hz with considerable amplitude, and the continuous ejection seems to exist at Pos.7. The less correlated behavior of the retarded regions means the scarce interaction between the neighboring vortex structure.

In the downstream sections at Sec.5 (Fig.12(c)) and Sec.6 (Fig.13(c)), the periodic characteristics in the velocity field become ambiguous because of the increased power of turbulent fluctuation as shown in Figs.9 and 11. It means that the boundary layer flow in these cross sections is approaching to the later stage of the transition, although the time-averaged structure of the Görtler vortices such as the spanwise pitch changes in the further downstream.

4. CONCLUSIONS

From the velocity measurements in the boundary layer flow on the rotating concave wall, the effects of system rotation on the occurrence and development of the Görtler vortices are examined experimentally. The results obtained from the present study are summarized in the following;

(1) For the rotating condition of N=0.012, Görtler type insta bility is enhanced, since both of the centrifugal force due to the wall curvature and the Coriolis force act toward the concave wall. Thus Görtler vortices start to occur in the boundary layer condition whose momentum thickness is thinner compared with the cases of N=0 and N=-0.012, and the shape of the retarded regions are uniform and their disposition are

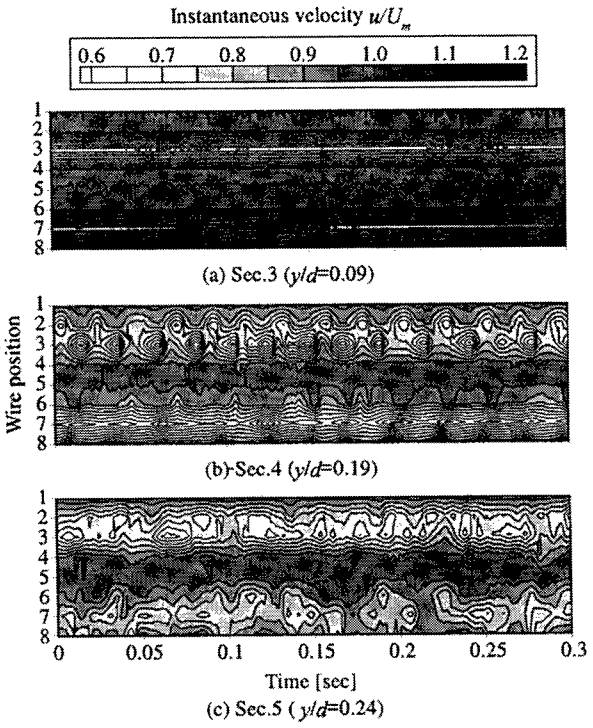

(a) Sec.3 (y/d=0.09)

(b) Sec.4 (y/d=0.19)

(c) Sec.5 (y/d=0.24)

Fig.12 Time traces of the longitudinal velocity in the region of C-1 (in Fig.3) for N=0.012

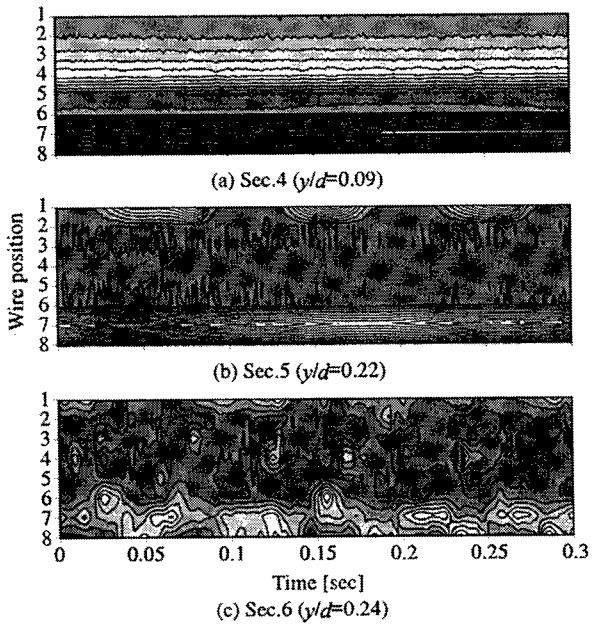

(a) Sec.4 (y/d=0.09)

(b) Sec.5 (y/d=0.22)

(c) Sec.6 (y/d=0.24)

Fig.13 Time traces of the longitudinal velocity in the region of C-2 (in fig.3) for N=-0.012

rather periodic in the spanwise direction.

(2) Görtler vortices grow in the transition stage of the boundary layer, and their pitch increases rapidly, although after the transition to turbulent the vortex structure is gradually getting weakened and the rate of the pitch increase falls. This tendency appears most remarkably when the centrifugal and Coriolis forces act in the opposite directions.

(3) The structure of Görtler vortices is kept steady state during the laminar condition, and moves to the unsteady state with the fluctuation of a certain frequency in the downstream section. As the transition proceeds further along the concave wall, the periodic fluctuations die out in Görtler vortices and the turbulent fluctuations dominate the flow structure.

NOMENCLATURE

d : Width of cross-section [mm]
h : Height of cross-section [mm]
H : Shape factor of boundary layer
N : Rotation rate (Eq.(1))
R : Radius of curvature for channel center-line [mm]
Re : Axial Reynolds number = $U_m d/\nu$
u : Instantaneous longitudinal velocity [m/s]
U : Time-averaged longitudinal velocity [m/s]
$\overline{U}$: Spanwise average of U [m/s]
u' : Rms value of fluctuating velocity component [m/s]
$\overline{u'}$: Spanwise averege of u' [m/s]
U_m : Free stream velocity at Sec.1 [m/s]
λ : Interval of vortices pair [mm]
θ : Momentum thickness of boundary layer [mm]
Ω : Rotational speed of channel [rad/s]

REFERENCES

Bradshaw, P., 1969, "The Analogy between Streamline Curvature and Buoyancy in Turbulent Shear Flow", *Journal of Fluid Mecanics*, Vol. 36, pp. 177-191.

Johnston, J. P., 1973, "The Suppression of Shear Layer Turbulence in Rotating Systems", Trans. ASME, *Journal of Fluids Engineering*, Vol. 95-1, pp. 229-239.

Kikuyama, K., Nishibori, K., Hara, S., 1987, "effects of System Rotation upon Turbulent Boundayry Layer on a Voncave Surface", *Proc. 6th Sympo. on Turbulent Shear Flows*, 1.4.1.

Koyama, H., Masuda, S., Ariga, I., and Watanabe, I., 1979, "Stabilizing and Destabilizing Effects of Coriolis Force on Two-dimensional Laminar and Turbulent Boundayr Layers", Trans. ASME, *Journal of Engng. Power*, Vol.101, pp. 23-31.

Matsson, O.J.E., and Alfredsson, P.H., 1990, "Curvature- and rotation-induced instabilities in channel flow", *Journal of fluid Mechanics*., Vol. 210, pp. 536-563.

Matubara, M., and Masuda, S., 1991, "Threedimensinal Instability in Rotating Boundary Layer", FED-Vol.114, Boundary layer Stability and Transition to Turbulence, ASME, pp.103-107.

Kikuyama, K., Hasegawa, Y., Yokoi, T., and Hirota, M., 1994, "Effects of Coriolis Force on Instability of Laminar Boundary Layer on a Concave Surface", ASME *Gas Turbine Conference*, Paper 94-GT-287, pp.1-8.

Aouidef, A., Wesfreid, J.E., and Mutabazi, I. 1992, "Coriolis Effects on Görtler Vortices in the Boundary-Layer Flow on Concave Wall", *AIAA Journal*, Vol. 30, pp.2779-2782.

Zebib. A., and Bottaro, A., 1993, "Goertler vortices with system rotarion: Linear theory", *Physics of Fluids A*, Vol. 5, pp. 1206-1210.

Kikuyama, K., Hasegawa, Y., and Ooe, T., 2000, "Effects of Channen Rotation and Wall Curvature on T-S Instability", *Proc. 3rd Int. Sympo. on Turbulent, Heat and Mass Transfer*, pp.669-676.

Kikuyama, K., Hasegawa, Y., Matsumoto, N., and Nishikawa, M., 2001, "Spanwise Rotation and Wall Curvature Effects on Instability of Boundary Layer", *Proc. 2nd Int. Sympo. on Turbulent and Shear Flow Phenomena*, pp. 73-78.